Cancer Research

Implication of Metastasis Suppressor *NM23-H1* in Maintaining Adherens Junctions and Limiting the Invasive Potential of Human Cancer Cells

Mathieu Boissan[1,2,3], Olivier De Wever[8], Floria Lizarraga[4,5], Dominique Wendum[1,2,6], Renaud Poincloux[4,5], Nicolas Chignard[1,2], Christèle Desbois-Mouthon[1,2], Sylvie Dufour[4,7], Béatrice Nawrocki-Raby[9], Philippe Birembaut[9], Marc Bracke[8], Philippe Chavrier[4,5], Christian Gespach[1,2], and Marie-Lise Lacombe[1,2]

Abstract

Loss of *NM23-H1* expression correlates with the degree of metastasis and with unfavorable clinical prognosis in several types of human carcinoma. However, the mechanistic basis for the metastasis suppressor function of *NM23-H1* is obscure. We silenced *NM23-H1* expression in human hepatoma and colon carcinoma cells and methodologically investigated effects on cell-cell adhesion, migration, invasion, and signaling linked to cancer progression. *NM23-H1* silencing disrupted cell-cell adhesion mediated by E-cadherin, resulting in β-catenin nuclear translocation and T-cell factor/lymphoid-enhancing factor-1 transactivation. Further, *NM23-H1* silencing promoted cellular scattering, motility, and extracellular matrix invasion by promoting invadopodia formation and upregulating several matrix metalloproteinases (MMP), including membrane type 1 MMP. In contrast, silencing the related *NM23-H2* gene was ineffective at promoting invasion. *NM23-H1* silencing activated proinvasive signaling pathways involving Rac1, mitogen-activated protein kinases, phosphatidylinositol 3-kinase (PI3K)/Akt, and src kinase. Conversely, *NM23-H1* was dispensable for cancer cell proliferation *in vitro* and liver regeneration in *NM23-M1* null mice, instead inducing cellular resistance to chemotherapeutic drugs *in vitro*. Analysis of NM23-H1 expression in clinical specimens revealed high expression in premalignant lesions (liver cirrhosis and colon adenoma) and the central body of primary liver or colon tumors, but downregulation at the invasive front of tumors. Our findings reveal that NM23-H1 is critical for control of cell-cell adhesion and cell migration at early stages of the invasive program in epithelial cancers, orchestrating a barrier against conversion of *in situ* carcinoma into invasive malignancy. *Cancer Res; 70(19); 7710–22. ©2010 AACR.*

Introduction

Metastasis suppressor genes, which exhibit a reduced expression in metastatic cancer cells, are defined by their ability to repress metastatic dissemination without impairing primary tumor growth (1). The first metastasis suppressor gene discovered was *NM23* (2). In humans, there are 10 genes belonging to the *NM23* gene family (also known as *NME* genes), of which the two most abundantly expressed are *NM23-H1* and *NM23-H2* that encode the A and B subunits of nucleoside diphosphate kinase (NDPK), respectively (3). Low NM23-H1 expression correlates with high metastatic potential in a subset of liver, colon, breast carcinoma, and melanoma human cohorts (4, 5). Ectopic expression of *NM23-H1* or *NM23-M1*, the murine ortholog of *NM23-H1*, reduces the metastatic behavior. Along this line, *NM23-H1* or *NM23-M1* overexpression downregulates anchorage-independent colonization, cell motility, and invasive potential (6). Furthermore, we have shown that *NM23-M1* null mice have a 2-fold greater incidence of lung metastases than wild-type mice when induced to form hepatocellular carcinoma (HCC; ref. 7).

The metastasis suppressor NM23-H1 is a multifunctional protein generating at least three enzymatic activities *in vitro*: a NDPK, a protein histidine kinase, and a recently characterized 3′-5′ exonuclease. Although the histidine protein kinase activity of NM23-H1 has been shown to correlate with suppression of motility in breast carcinoma cell lines *in vitro* (8), the concept has yet to be addressed directly using models of

Authors' Affiliations: [1]UPMC Université Paris 06; [2]INSERM UMR_S938, Centre de Recherche Saint-Antoine; [3]AP-HP, Hôpital Tenon, Service de Biochimie et Hormonologie; [4]Institut Curie, Centre de Recherche; [5]CNRS, UMR144, Dynamique de la Membrane et du Cytosquelette; [6]APHP, Hôpital Saint-Antoine, Service d'Anatomie Pathologique; [7]CNRS, UMR144, Bases Mécaniques et Moléculaires de l'Adhérence et de la Migration Cellulaires, Paris, France; [8]Laboratory of Experimental Cancer Research, Gent, Belgium; and [9]INSERM UMR_S903, CHU Maison Blanche, Université de Reims Champagne-Ardenne, Reims, France

Note: Supplementary data for this article are available at Cancer Research Online (http://cancerres.aacrjournals.org/).

C. Gespach and M-L. Lacombe contributed equally to this work.

Corresponding Author: Mathieu Boissan, UPMC, CdR Saint-Antoine UMR_S938, 27 rue Chaligny, 75571 Paris Cedex 12, France. Phone: 33-1-40-01-13-21; Fax: 33-1-40-01-14-32; E-mail: mathieu.boissan@inserm.fr.

doi: 10.1158/0008-5472.CAN-10-1887

metastatic growth. A role for the NDPK activity in metastasis suppression has been challenged (9–11). It was shown that the H118F mutant lacking NDPK activity exhibited compromised metastasis suppressor activity. However, it should be stressed that mutations targeting NDPK activity can preclude other enzymatic and signaling functions and interactions of NM23-H1 with its molecular partners. Finally, Zhang and colleagues provided the first demonstration that the 3′-5′ exonuclease activity was necessary for the NM23-H1 metastasis suppressor function (11).

Family members of the Rho-GTPases have been recognized to play a key role in the actin cytoskeleton dynamics required for cancer cell migration and invasion. Some reports suggest that NM23-H1 inhibits cell migration and cancer metastasis by modulating the activity of members of the Rho small GTPase family. NM23-H1 negatively regulates Rac1 and Cdc42 by interacting with their specific exchange factors Tiam1 and Dbl-1, respectively (12, 13). NM23-H1 was shown to reduce transcription of the *EDG2* gene, which encodes the lysophosphatidic acid receptor involved in metastasis and connected with the Rho-ROCK axis (14). NM23-H1 also represses the Ras/mitogen-activated protein kinase (MAPK) and transforming growth factor-β signaling pathways involved in cancer invasion (15, 16). In addition, the rat homologue of NM23-H1 inhibits expression of the gene encoding the matrix metalloproteinase MMP-2, a key effector of cancer invasion (17). Despite these observations, our understanding of the cellular and molecular mechanisms underlying the antimetastatic activity of *NM23-H1*/*NM23-M1* remains sketchy.

We therefore sought to determine the role of *NM23-H1* on the initial steps of the metastatic dissemination initiated by local invasion of extracellular matrices by cancer cells in the context of the progression of human hepatocellular and colorectal carcinomas. Here, we show a pivotal role for *NM23-H1* in the maintenance of E-cadherin–mediated intercellular adhesion and limitation of the invasive potential, and identify several cellular and molecular mechanisms underlying these processes.

Materials and Methods

Cell culture

Human liver (HepG2), colon (HCT8/S11), and breast (MDA-MB-231) cancer cell lines were maintained in DMEM supplemented with 10% fetal bovine serum (FBS). Human hepatoma cell lines PLC/PRF/5 and Mahlavu were maintained in MEM containing Earle's salts, 1% nonessential amino acids, 1 mmol/L sodium pyruvate, and 10% FBS. Primary human hepatocytes were isolated and cultured as previously reported (18).

Authentication of cell lines

Human breast adenocarcinoma MDA-MB-231 cells and hepatoma HepG2 cells were obtained from the American Type Culture Collection. MDA-MB-231 cells are characterized by cytogenetic analysis and expression of the WNT7B oncogene. HepG2 cells express 3-hydroxy-3-methylglutaryl-CoA reductase and hepatic triglyceride lipase activities. These cells show decreased expression of apoA-I mRNA and increased expression of catalase mRNA in response to gramoxone. Finally, there is no evidence of a hepatitis B virus genome in these cells. The human colon cancer cell line HCT8/S11 was initially described by Vermeulen and colleagues (19). Several nucleotide sequences of integrated hepatitis B virus DNA have been found in the genome of the PLC/PRF/5 cell line (20). In particular, an insertional activation of the *mevalonate kinase* gene by hepatitis B virus DNA has been reported in the PLC/PRF/5 cell line (21). Mahlavu cells have no sequences of integrated hepatitis B virus DNA but presented homozygous deletion of the *PTEN* gene (22).

Cell aggregation, invasion, wound healing, cell dispersion, fluorescent gelatin degradation, and quantification of invadopodia

Slow and fast aggregation assays were performed as reported (23). Native type I collagen and Matrigel invasion assays were performed as described earlier (24, 25). Migration of HCT8/S11 cells was evaluated by a wound-healing migration assay (26). Cellular spatial distribution was characterized and quantified as described (27). Fluorescent gelatin degradation assay and quantification of invadopodia were performed as reported previously (28).

Videomicroscopy

HepG2 cells were tracked for 24 hours and four parameters were analyzed: mean speed of migration was calculated by dividing the total distance of migration by the time of the experiment (24 hours); mean velocity was evaluated for cells only exhibiting a movement between two successive acquisitions (5 minutes) during the experiment; maximal velocity was the highest velocity observed between two successive acquisitions; and the migration frequency corresponded to how frequently the cells moved between two successive acquisitions during the course of the experiment. This was done for at least 20 cells per field, in four random fields for each condition.

Statistical analysis

Microsoft Excel software was used to calculate mean, SD, and SEM and to perform Student's t test. SPSS version 12.0 software (IBM) was used to perform all other statistical tests of significance. For the fast aggregation assay, statistical significance was assessed by the Kolmogorov-Smirnov test, and values >20 were considered to be statistically significant (26). Degradation index was analyzed by using a Levene test to determine whether there was homoscedasticity of variance, followed by an unpaired Student's t test with Holm adjustment (29). The χ^2 test was used for comparison of groups in the type I collagen invasion assay when counting the number of noninvasive and invasive cells in 10 microscopic fields, and in the fluorescent gelatin degradation assay when determining the percentage of cells with invadopodia in at least 20 random microscopic fields. For all other comparisons between two groups, we performed an unpaired Student's t test. In all tests, the level of statistical significance was set at $P < 0.05$.

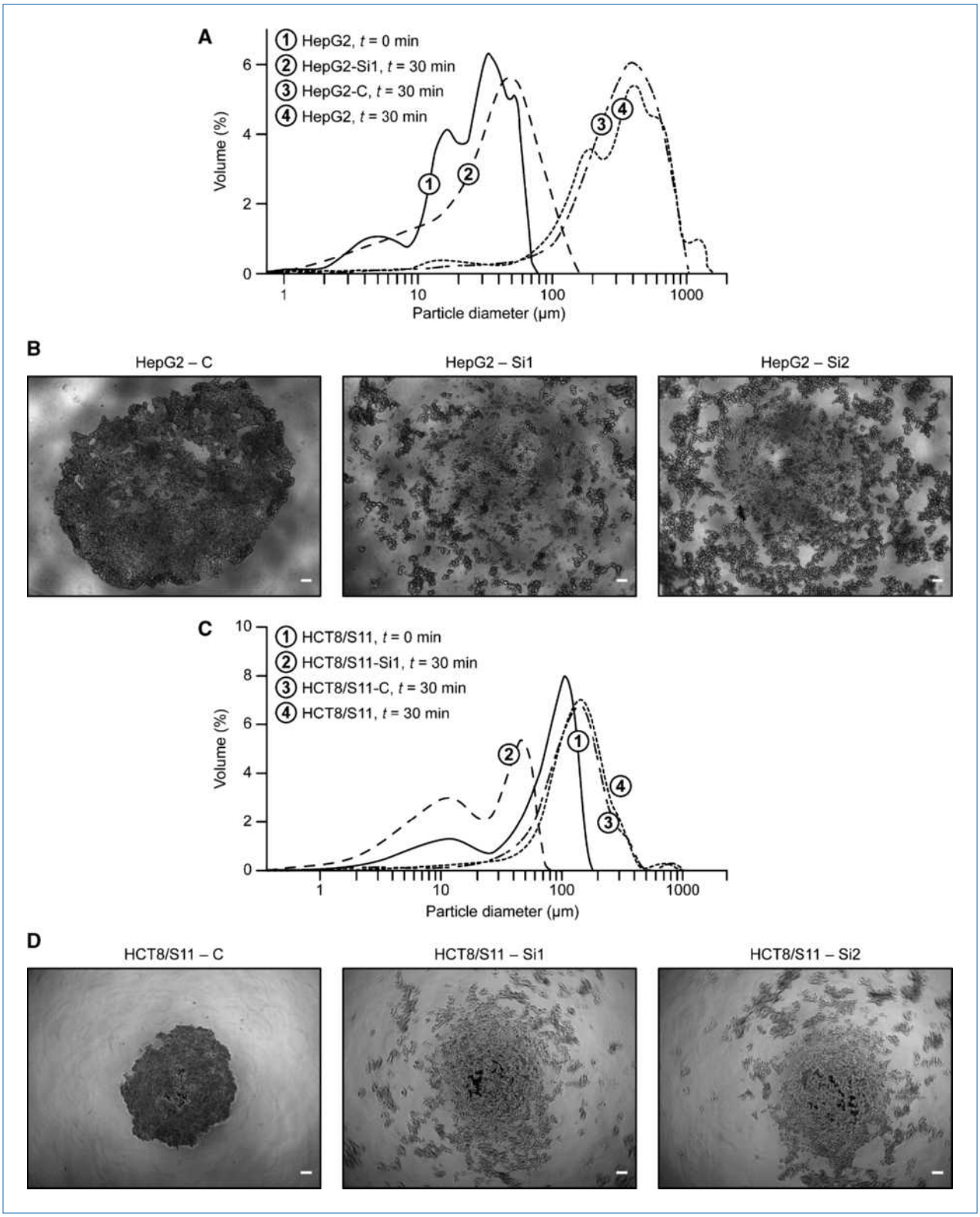

Figure 1. Disruption of intercellular adhesion by *NM23-H1* silencing. A and C, in fast aggregation assays, parental, control siRNA (C), and Si1-silenced cells were allowed to aggregate in a gyratory shaker. Cell aggregation was measured by counting particle size after 0- and 30-min incubation. Each assay was repeated three times. B and D, slow aggregation assays were performed by seeding control and silenced (Si1 and Si2) cells on top of a gelified agar medium. Aggregate formation was scored after 24-h incubation at 37°C. Each assay was repeated three times. Scale bar, 100 μm.

Results

Expression and silencing of *NM23-H1* in human cancer cell lines

NM23-H1 levels were analyzed by Western blotting of extracts of human liver, colon, and breast cancer cell lines with polyclonal antibodies specific for NM23-H1 (Supplementary Fig. S1A). NM23-H1 protein was barely detectable in normal human hepatocytes in primary culture. By contrast, we observed substantial expression of NM23-H1 in the hepatoma cell lines HepG2, PLC/PRF/5, and Mahlavu. HepG2 and PLC/PRF/5 hepatoma cells and HCT8/S11 colon cancer cells, all of which displayed high levels of NM23-H1, were not invasive in native type I collagen, the major element of the stromal matrix in human solid tumors. Conversely, the highly invasive MDA-MB-231 breast carcinoma and Mahlavu cells expressed low levels of NM23-H1. To validate the inverse relationship between NM23-H1 protein levels and invasive behavior, we selectively silenced *NM23-H1* with two independent siRNAs (Si1 and Si2) in HepG2, PLC/PRF/5, and HCT8/S11 cells. As a consequence, both *NM23-H1* mRNA and protein levels were highly reduced (Supplementary Fig. S1B and C). Expression of the closely related NM23-H2 isoform remained unchanged on *NM23-H1* silencing, showing that the regulation of NM23-H1 and NM23-H2 protein levels is independent. In addition, *NM23-H1* silencing reduced by 20% and 15% the total NDPK activity in HepG2 and HCT8/S11 cells, respectively, supporting the notion that the NDPK intrinsic activity of NM23-H1 only represents a minor fraction of the global cellular NDPK activity in these cells (Supplementary Fig. S1D).

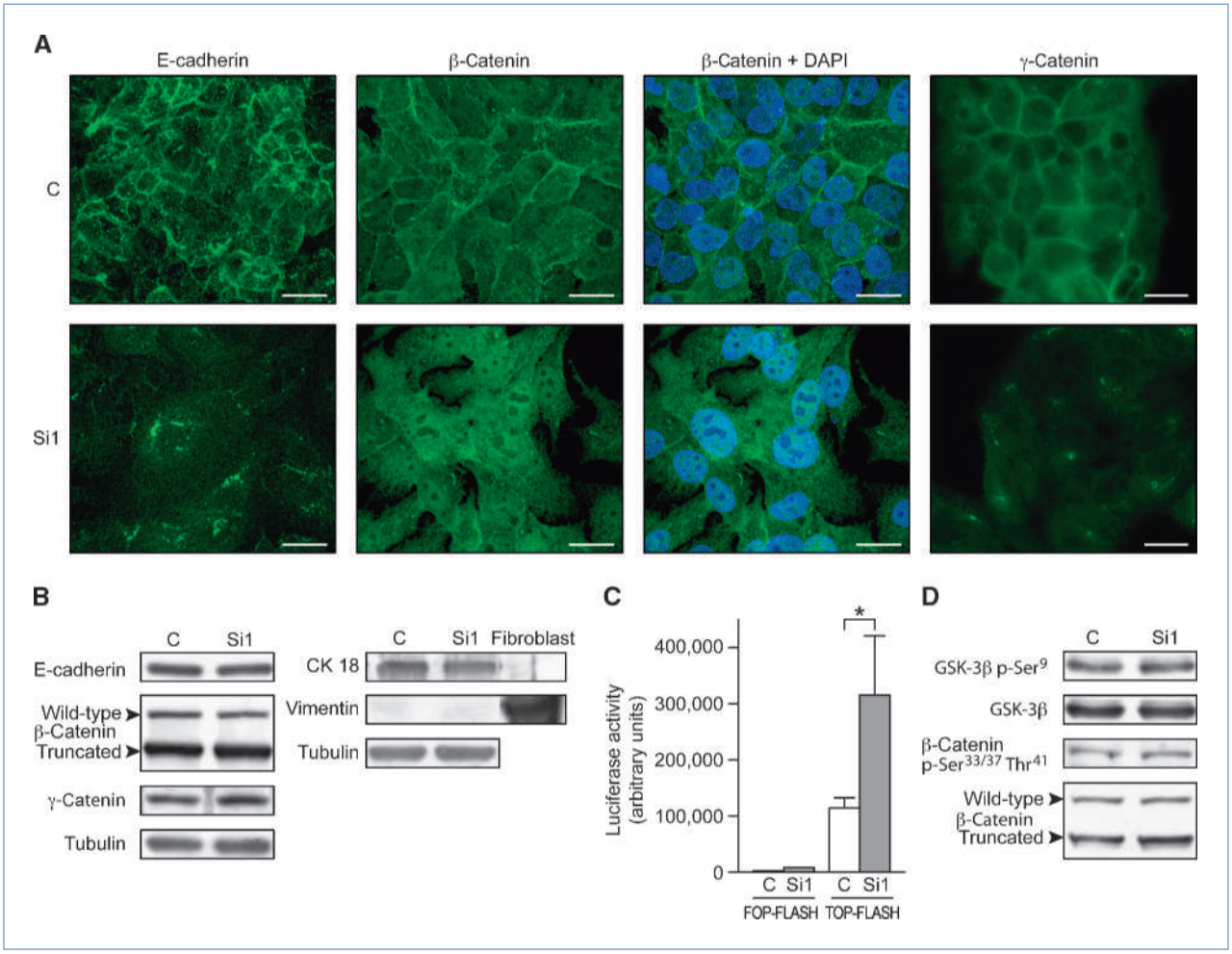

Figure 2. Disassembly of adherens junctions and β-catenin–TCF/LEF-1 transactivation by *NM23-H1* silencing. A, immunostaining of E-cadherin, β-catenin, and γ-catenin in control and silenced (Si1) HepG2 cells analyzed 48 h after transfection by confocal microscopy. Scale bar, 20 μm. B, Western blotting of whole-cell lysates prepared from control and silenced HepG2 cells 48 h after transfection for the expression of E-cadherin, β-catenin, and γ-catenin (left) and CK 18 and vimentin (right). Skin fibroblast extracts were used as a negative control for CK 18 and a positive control for vimentin. C, control and silenced HepG2 cells 48 h after transfection were transiently transfected with the FOP-FLASH and TOP-FLASH luciferase reporter constructs. After 24 h, luciferase activity was determined. Columns, mean of three independent experiments, each performed in duplicate; bars, SEM. *, $P < 0.05$ versus control cells. D, phosphorylated levels of GSK-3β (Ser^{9}) and β-catenin ($Ser^{33/37}$ Thr^{41}) were determined by Western blotting in control and silenced HepG2 cells.

NM23-H1 silencing induces epithelial cancer cell scattering

Next, we investigated the effect of *NM23-H1* silencing on cell scattering, which recapitulates the early steps of the metastatic cascade. HepG2 cells are normally organized as epithelioid clusters. *NM23-H1* silencing induced extensive scattering of the cells and a marked change of the morphology of cells displaying more and longer cytoplasmic extensions than control cells (Supplementary Fig. S2A). The cell cohesion index was quantified in a cell dispersion assay (27), revealing that silencing of *NM23-H1* resulted in a more random spatial distribution of the cells compared with controls, in agreement with the cell scattering phenotype (Supplementary Fig. S2B and C). The morphologic changes in silenced HCT8/S11 cells were less marked than in HepG2 cells (data not shown). However, when seeded on native type I collagen, silenced HCT8/S11 cells formed numerous cellular extensions compared with control cells (Supplementary Fig. S2D, top). As is the case in HepG2 cells, *NM23-H1* silencing induced PLC/PRF/5 cell scattering (Supplementary Fig. S2D, bottom). This phenotype was observed at 2 to 7 days after transfection when NM23-H1 depletion was maximal in HepG2 cells, whereas it disappeared at day 14 when silenced cells had recovered control levels of NM23-H1 (Supplementary Fig. S3; data not shown).

NM23-H1 silencing impairs intercellular adhesion

The acquisition of a scattered phenotype is often associated with alterations in intercellular adhesion. We therefore investigated the effect of *NM23-H1* silencing on the cell-cell adhesion properties of HepG2 and HCT8/S11 cells. When cluster size was measured by using the fast aggregation assay, the parental and control siRNA cells spontaneously formed aggregates, in sharp contrast to the silenced cells showing no cell-cell aggregation (Fig. 1A and C). Likewise, in the slow aggregation assay, control cells grown on soft agar formed compact islands, whereas silenced cells did not (Fig. 1B and D).

NM23-H1 silencing disrupts adherens junction complexes and activates the Wnt pathway

Both E-cadherin and catenins are involved in establishing and maintaining cell-cell adhesion in epithelial cells. E-cadherin, β-catenin, and γ-catenin were highly expressed at cell-cell contacts of control HepG2 cells. *NM23-H1* silencing resulted in a marked reduction of E-cadherin/catenin staining at cell-cell contacts, and a redistribution of β-catenin from the cell surface into the cytoplasm and nucleus (Fig. 2A). However, total levels of these proteins were unchanged between control and silenced cells (Fig. 2B). Similarly, no change in E-cadherin/β-catenin protein levels was observed in silenced HCT8/S11 cells (data not shown). These results indicate that depletion of NM23-H1 results in concerted delocalization of plasma membrane junctional proteins, without altering their expression levels. These adherens junction defects, which were not associated with loss of cytokeratin 18 (CK 18) and gain of vimentin, likely explain the scattering and reduced cell-cell adhesion we observed in silenced cells, suggesting progression to a partial epithelial-mesenchymal transition (EMT; Fig. 2B). Accordingly, *NM23-H1* silencing was not associated with upregulation of the E-cadherin repressors Snail, Slug, and Twist (Supplementary Fig. S4).

To examine the functional effect of the translocation of β-catenin into the nucleus in silenced HepG2 cells, we measured T-cell factor/lymphoid-enhancing factor-1 (TCF/LEF-1) transcriptional activity with the TOP-FOP luciferase reporter assay. As expected, the β-catenin signaling pathway was constitutively activated in control HepG2 cells. Indeed, these cells express two β-catenin isoforms: the longer isoform is regulated by glycogen synthase kinase-3β (GSK-3β)–mediated phosphorylation, whereas the shorter form lacks these regulatory sites, leading to stabilization of this truncated β-catenin and partial activation of the Wnt pathway (30). However, on *NM23-H1* silencing, this pathway was further hyperactivated 3-fold (Fig. 2C). In the silenced cells, however, there was no change in the phosphorylation levels of both GSK-3β (at Ser^{9}) and wild-type β-catenin (at the GSK-3β–dependent phosphorylation sites $Ser^{33}/Ser^{37}/Thr^{41}$; Fig. 2D). Collectively, these observations indicate that *NM23-H1* silencing in HepG2 cells induces β-catenin–TCF/LEF-1 transactivation through a GSK-3β–independent mechanism.

NM23-H1 silencing induces cellular motility, directional migration, and reorganization of the actin cytoskeleton

Acquisition of a scattered and motile phenotype by cancer cells is an important prerequisite for invasion and metastasis. The motility of cells with altered NM23-H1 expression was quantified for the first time by videomicroscopy (Fig. 3A). Silencing in HepG2 cells increased the mean speed of migration by >3-fold and the migration frequency (Supplementary Movies S1 and S2). In addition, two other quantitative parameters, including mean and maximal velocity (see Materials and Methods), were both significantly increased by *NM23-H1* silencing (data not shown). Trajectories of individual silenced cells were persistent, in contrast to the highly restricted motility of control cells exhibiting much shorter trajectories (Fig. 3A). Along the same line, using a wound-healing assay to measure the directional migration of HCT8/S11 cells, we observed that healing was complete in silenced cells, whereas wounding was still apparent in control cells (Fig. 3B; Supplementary Fig. S5). Remarkably, *NM23-H1* silencing was accompanied by remodeling of the actin cytoskeleton as shown by the formation of filopodia-like structures on the free surface of the cells (Fig. 3C). Actin cytoskeletal reorganization accompanying motility is regulated by Rho-GTPases. In the silenced cells 72 hours after transfection, levels of active GTP-bound Rac1 increased compared with the control cells (Fig. 3D, left); however, this was not accompanied by induction of the constitutively active Rac1b isoform (Fig. 3D, right), which is an alternatively spliced variant of Rac1 involved in promoting cancer cell invasion (31). In summary, *NM23-H1* silencing triggered a migratory phenotype in the two cell models.

Induction of the invasive phenotype and oncogenic pathways by silencing of *NM23-H1*

Because the ability to breach extracellular matrix barriers is critical for metastasis, we assessed the effect of *NM23-H1* silencing on the capacity of the cell to invade a three-dimensional

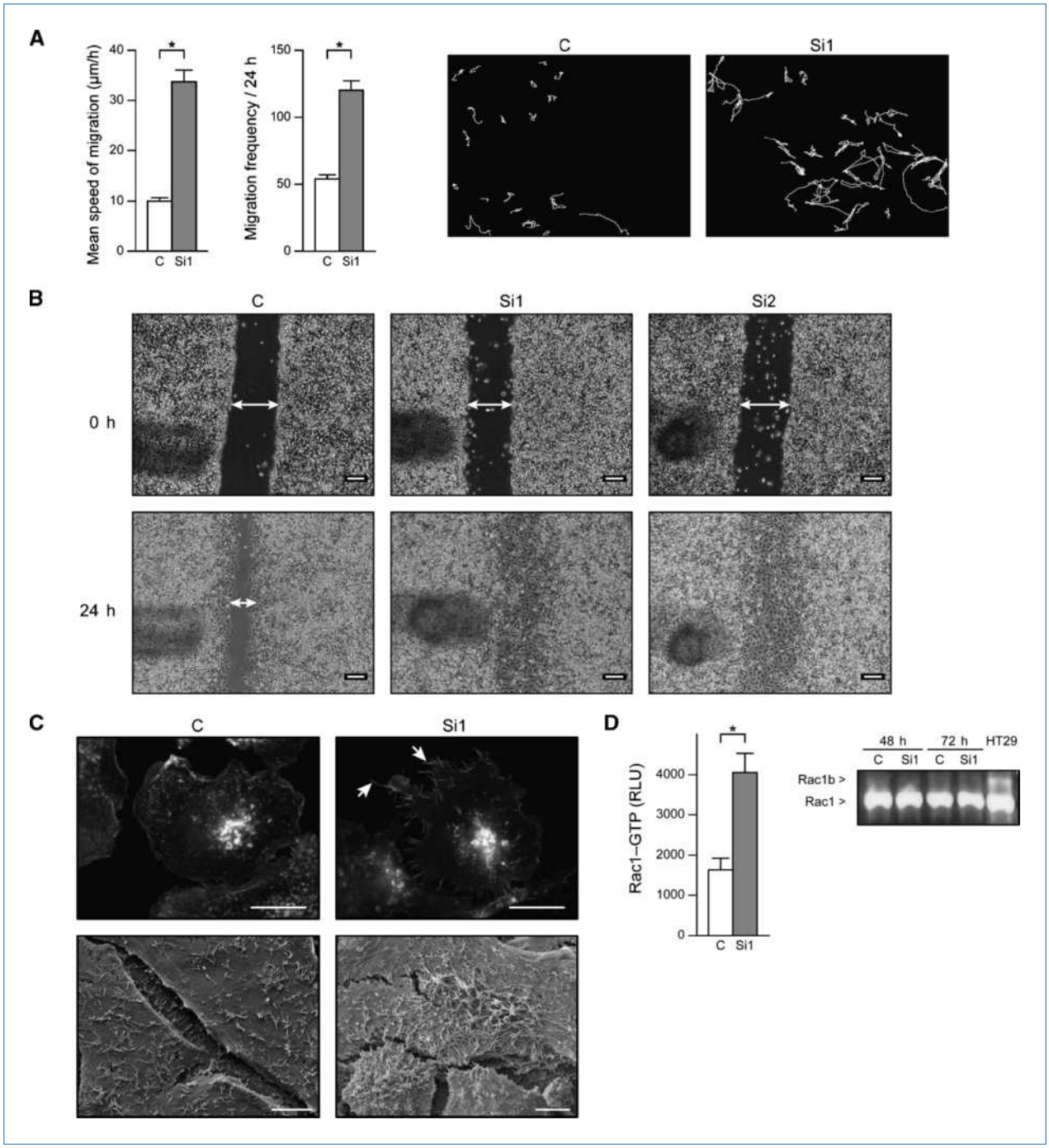

Figure 3. *NM23-H1* silencing promotes cellular motility, facilitates wound healing, and induces remodeling of the actin cytoskeleton architecture with filopodia-like structures and Rac1 activation. A, the random motility of control and silenced (Si1) HepG2 cells 48 h after transfection was tracked by videomicroscopy over 24 h. The mean speed of migration and migration frequency were measured as described in Materials and Methods. Columns, mean; bars, SEM. *, $P < 0.05$ versus control cells. The trajectories of control and silenced HepG2 cells were computed from images recorded for 24 h at 5-min intervals. Twenty cell tracks are shown for each condition. B, confluent monolayers of control and silenced (Si1 and Si2) HCT8/S11 cells were wounded and then cultured for 24 h at 37°C. Representative photographs at 0 and 24 h after wounding are shown. Scale bar, 200 μm. C, top, immunostaining with phalloidin of control and silenced (Si1) HepG2 cells 48 h after transfection visualized under a confocal laser microscope. Arrows show filopodia-like structures. Similar effects were observed with the Si2 siRNA (data not shown). Scale bar, 20 μm. Bottom, scanning electron microscopy of the same cells. Scale bar, 5 μm. D, left, ELISA-based GTPase activation assay of Rac1 in control and silenced HepG2 cells 72 h after transfection. Columns, mean of three independent experiments, each performed in triplicate; bars, SEM. *, $P < 0.05$ versus control cells. Right, Rac1 and Rac1b expression assayed by reverse transcription-PCR in control and silenced HepG2 cells 48 and 72 h after transfection. Rac1 mRNA is expressed at similar levels in all samples. The Rac1b splice variant is seen only in HT29 cells, used as positive control.

matrix of native type I collagen (Fig. 4A). *NM23-H1* silencing induced a cell-autonomous invasive phenotype in HepG2, HCT8/S11, and PLC/PRF/5 cells. Furthermore, silencing of *NM23-H1* increased invasion in Matrigel, a basement membrane extract (Fig. 4A). To establish the specificity of the *NM23* family member *NM23-H1* as a regulator of cancer cell invasion, we specifically silenced the *NM23-H2* homologue by using the Si1′ and Si2′ siRNAs. Both Si1′ and Si2′ strongly reduced NM23-H2 protein levels without altering NM23-H1 expression (Supplementary Fig. S6A). Importantly, *NM23-H2* silencing did not promote invasion (Supplementary Fig. S6B), although it strongly reduced the total NDPK activity by 52% and 38% in HepG2 and HCT8/S11 cells, respectively (Supplementary Fig. S6C).

Taken together, our findings support the notion that the NDPK intrinsic activity of NM23-H1 might be sufficient to support functional E-cadherin–dependent adherens junctions. In addition, our data suggest that other NDPK isoforms are not able to rescue the depletion of NM23-H1, and therefore support a major role for this NDPK in regulating cancer cell-cell adhesion and the early steps of the invasive process. Finally, our data establish the specific role of *NM23-H1* as a general negative regulator of cancer cell invasion irrespective of the composition/organization of the matrix environment. Next, we assessed the proinvasive activity of serum-free conditioned medium (CM) prepared from control and *NM23-H1*–silenced cells of both HepG2 and HCT8/S11 cell lines in the native type I collagen. All CM had no effect on the invasive potential of untreated HepG2 and HCT8/S11 cells (data not shown), indicating that the invasive phenotype induced by *NM23-H1* silencing in the two cell models is initiated by cell-associated proinvasive signals and not secreted factors.

We therefore analyzed the possible contribution of several proinvasive pathways to the invasive capacity of silenced cells by using specific inhibitors of intracellular signaling components. Invasion of type I collagen matrices by silenced HepG2 cells was strongly inhibited by selective pharmacologic inhibitors of extracellular signal-regulated kinase (ERK) 1/2 (PD098059), p38 (SB203580), c-Jun NH_2-terminal kinase (JNK; SP600125), PI3K (wortmaninn), the Rho-GTPases (C3T), the ROCK kinase (Y27632), and src (PP1 and M475271) signaling pathways (Fig. 4B; data not shown). By contrast, the invasive potential was insensitive to inhibitors of NF-κB and mammalian target of rapamycin (mTOR; CAPE and rapamycin, respectively), as well as to inhibitors of phospholipase C (PLC; U73122), $G\alpha_0/G\alpha_i$ G proteins (pertussis toxin), and protein kinase A (PKA; KT5720) pathways. Similar responses were observed in silenced HCT8/S11 cells (Fig. 4C). These effects correlated with hyperactivation of ERK1/2, p38, and JNK, as judged by their phosphorylated states in silenced HepG2 cells (Fig. 4D). We found consistent activation of Akt and p70/p85 S6 kinase (S6K), two downstream effectors of PI3K, and concomitant downregulation of PTEN protein levels in silenced HepG2 cells. By contrast, PTEN protein levels remained unchanged in silenced HCT8/S11 cells despite increased Akt phosphorylation, implying cell type–specific differences in the response to *NM23-H1* silencing (Fig. 4D). In the three cancer cell lines (HepG2, HCT8/S11, and PLC/PRF/5), Akt hyperactivation was transient and appeared before Rac1 activation in HepG2 cells (Supplementary Fig. S7). Consistently, the highly invasive breast and hepatoma cell lines MDA-MB-231 and Mahlavu displayed high levels of phosphorylated Akt in comparison with the noninvasive cell lines HepG2, PLC/PRF/5, and HCT8/S11 (Supplementary Fig. S8). Thus, *NM23-H1* loss and silencing correlates with the invasive potential and Akt hyperactivation.

NM23-H1 silencing promotes pericellular MMP activity

With regard to the effects of NM23-H1 depletion on cell-associated invasive signals, we investigated the contribution of pericellular matrix degradation activity of silenced cells. First, we addressed the effect of *NM23-H1* silencing on gelatin degradation and formation of invadopodia, defined as actin-driven membrane protrusions endowed with matrix proteolytic activity. HepG2 cells were plated on coverslips coated with a thin layer of fluorescently labeled gelatin matrix. Local proteolytic activity was identified by the appearance of dark areas lacking fluorescence (Fig. 5A and B). Cells were considered positive for invadopodia if they showed actin/cortactin-rich puncta overlying areas of gelatin degradation (Fig. 5B, arrowheads). Silencing stimulated gelatin degradation (Fig. 5C, left), with ~20% of silenced cells forming invadopodia, whereas these structures were barely visible in control cells (Fig. 5C, right). Because invadopodia are dynamic structures, some areas of gelatin degradation were observed that were no longer associated with invadopodia (Fig. 5B, arrows). To determine whether *NM23-H1* silencing–induced invasion was dependent on MMP, we measured the invasion of native type I collagen by silenced cells in the presence of the general MMP inhibitor GM6001. As shown in Supplementary Fig. S9, GM6001 strongly inhibited invasion induced by *NM23-H1* silencing. These effects correlated with increased expression of membrane type 1 MMP (MT1-MMP), the key invadopodial MMP, in silenced cells (Fig. 5D, top). In agreement with these data, invasion in native type I collagen was inhibited by ectopic expression of a catalytic domain deletion mutant of MT1-MMP (MT1-Δcat) in silenced cells. Conversely, overexpression of the proteolytically active form of MT1-MMP (MT1-wt) promoted invasion in control cells and led to further increased invasion of silenced cells (Fig. 5D, bottom).

Role of NM23-H1/NM23-M1 in cancer cell proliferation and survival

To investigate the relationship between NM23-H1 expression and cell proliferation, the effect of *NM23-H1* silencing was determined on anchorage-dependent and anchorage-independent growth. As analyzed by flow cytometry, the percentage of cells in each phase of the cell cycle was identical in control and silenced cells (Supplementary Fig. S10A). Accordingly, protein levels of the cell cycle marker proliferating cell nuclear antigen (PCNA) remained identical in both conditions (data not shown). Furthermore, the number and size of HepG2 colonies formed in soft agar were similar in control and silenced cells (Supplementary Fig. S10B; data not shown). Thus, *NM23-H1* silencing did not provide an intrinsic proliferative advantage to epithelial cancer cells.

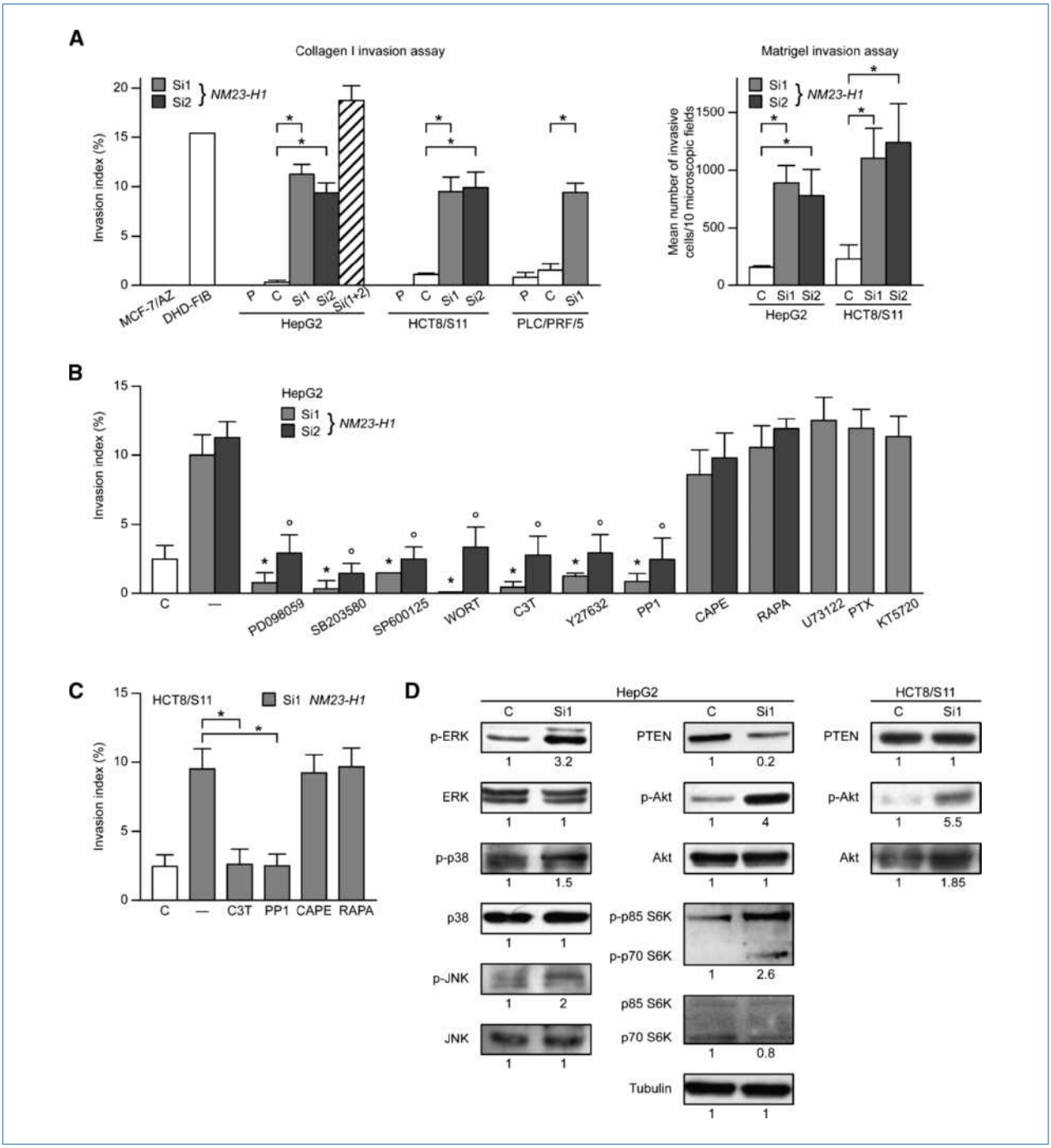

Figure 4. The invasive phenotype induced by *NM23-H1* silencing depends on MAPK, PI3K/Akt, Rho/ROCK, and src signaling. A, left, parental (P), control siRNA (C), and *NM23-H1*–silenced (Si1 and Si2) cells were tested for their ability to invade native type I collagen in a 24-h invasion assay. MCF-7/AZ human mammary carcinoma cells and DHD-FIB rat colon myofibroblasts were used as negative and positive controls, respectively. Columns, mean of five independent experiments; bars, SEM. *, $P < 0.05$ versus control cells. Right, cells, as in the left, were tested for their ability to invade a Matrigel matrix in a 48-h invasion assay. Columns, mean of 10 independent fields; bars, SD. Each experiment was repeated twice. *, $P < 0.05$ versus control cells. B and C, *NM23-H1*–silenced (Si1 and Si2) cells were tested for their ability to invade native type I collagen in the presence of pharmacologic inhibitors of ERK1/2 (PD098059, 50 μmol/L), p38 (SB203580, 10 μmol/L), JNK (SP600125, 2 μmol/L), PI3K (wortmannin, 10 nmol/L), Rho-GTPases (C3T exoenzyme, 5 μg/mL), ROCK (Y27632, 1 μmol/L), src (PP1, 10 μmol/L), NF-κB (CAPE, 10 μmol/L), mTOR (rapamycin, 20 nmol/L), PLC (U73122, 1 μmol/L), $G\alpha_0/G\alpha_i$ G proteins (pertussis toxin, 0.2 μg/mL), and PKA (KT5720, 1 μmol/L). Columns, mean of four independent experiments; bars, SEM. * and °, $P < 0.05$ versus untreated Si1- and Si2-silenced cells, respectively. D, whole-cell lysates of control and *NM23-H1*–silenced cells were analyzed 48 h after transfection by Western blotting with specific antibodies against the phosphorylated forms of ERK1/2, p38, JNK, Akt, and p70/p85 S6K and against PTEN and tubulin. The intensity of immunoreactive bands in silenced cells was quantified by densitometry relative to control cells.

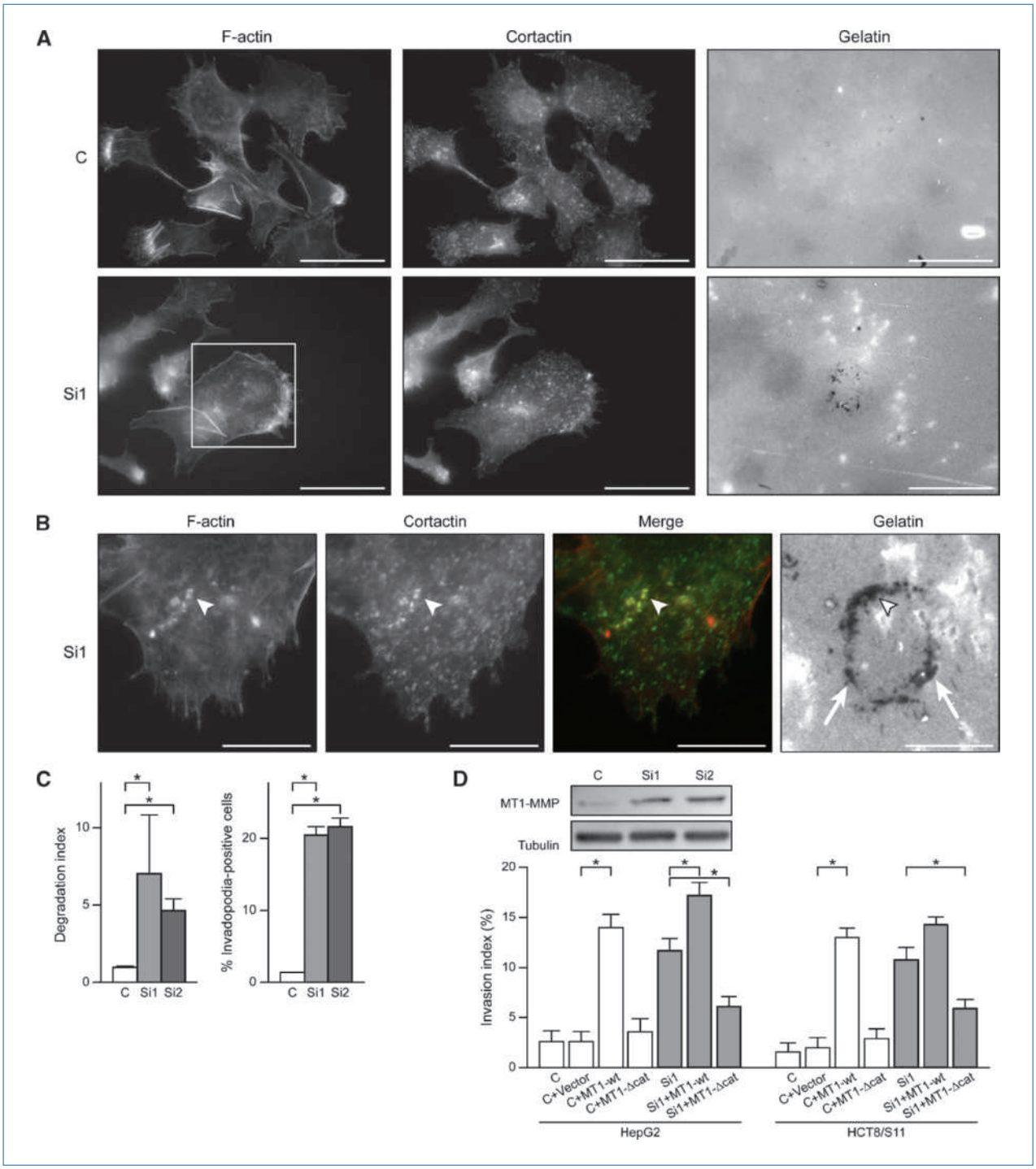

Figure 5. Gelatin degradation, invadopodia formation, and MT1-MMP expression are induced by *NM23-H1* silencing. A, control and silenced HepG2 cells 48 h after transfection were incubated for 36 h on fluorescent gelatin, fixed, and stained for F-actin and cortactin. Representative images are shown. Scale bar, 40 μm. B, higher magnification of silenced HepG2 cells stained for F-actin and cortactin. In the merged image, F-actin is red and cortactin is green. Invadopodia positive for both markers overly regions of degraded gelatin (arrowheads). Areas of degradation, which were no longer associated with invadopodia, are shown (arrows). Scale bar, 20 μm. C, graphs depicting the gelatin degradation index and the percentage of invadopodia-positive cells in control and silenced (Si1 and Si2) HepG2 cells. Columns, mean of three independent experiments, with at least 20 random fields analyzed per experiment; bars, SEM. *, $P < 0.05$ versus control cells. D, top, MT1-MMP expression analyzed by Western blotting of whole-cell lysates prepared from control and silenced (Si1 and Si2) HepG2 cells 72 h after transfection. Bottom, control and silenced cells were transfected with expression vectors encoding full-length MT1-MMP (MT1-wt) or a form mutated in its catalytic domain (MT1-Δcat) and then tested for their invasive capacity in native type I collagen. Columns, mean of three independent experiments; bars, SEM. *, $P < 0.05$.

To confirm that NM23-H1 depletion had no effect on cellular proliferation, we performed partial hepatectomy in *NM23-M1*$^{-/-}$ mice and analyzed liver regeneration. Hepatocyte proliferation, evaluated by immunostaining of nuclear Ki67, was identical in wild-type and NM23-M1$^{-/-}$ mice (Supplementary Fig. S10C, left). In wild-type mice, we observed a strong increase in NM23-M1 protein levels at 40 and 48 hours (3-fold increase) after hepatectomy, followed by a drastic reduction at 96 hours, when hepatocyte proliferation strongly decreased (Supplementary Fig. S10C, right). By contrast, NM23-M2 expression increased to a lesser extent in both wild-type (1.79-fold increase) and *NM23-M1*$^{-/-}$ (1.70-fold increase) mice. These results show that ablation of *NM23-M1* is compatible with liver regeneration and that NM23-M1, despite a marked increase in its expression, is dispensable for the growth of nontransformed hepatocytes *in vivo*. These findings strongly suggest a compensatory mechanism by the very highly homologous NM23-M2 isoform, even if its expression in the *NM23-M1*$^{-/-}$ mice is not further increased compared with the wild-type mice. Therefore, NM23-H1/NM23-M1 is not required for epithelial cell proliferation *in vitro* and *in vivo*. The mechanisms involved in the survival of invasive and metastatic cancer cells during cancer progression and chemotherapy contribute to drug resistances in primary tumors and metastases. Chemoresistances are associated with poor prognosis for cancer patients. We examined the effect of *NM23-H1* silencing on apoptosis induced by the anticancer agents camptothecin and etoposide as topoisomerase I and II inhibitors, respectively, in HepG2 cells. *NM23-H1* silencing induced resistance to apoptosis triggered by these agents (Supplementary Fig. S10D).

NM23-H1 and NM23-H2 expression in human hepatocellular and colorectal carcinoma

Immunoblotting analysis of seven human HCC specimens using selective anti–NM23-H1 antibodies revealed high NM23-H1 levels in six of seven HCC specimens when compared with nontumoral liver tissue (Supplementary Fig. S11A, left). Study of the same specimens with specific anti–NM23-H2 antibodies showed that NM23-H2 levels were increased in five of seven HCC compared with their paired controls. Likewise, in two of three cirrhotic liver samples (samples 2 and 3), we found higher levels of NM23-H1 and NM23-H2 than in control liver tissue (Supplementary Fig. S11A, right). We confirmed the increase of NM23-H1 in cirrhotic liver tissue and even at higher levels in tumor nodules by immunohistochemistry (Supplementary Fig. S11B). NM23-H1 labeling was heterogeneous within a given liver tumor sample, suggesting that NM23-H1 expression may be lost in some areas of the tumor (Supplementary Fig. S11B, right, asterisk). In HCC, NM23-H1 staining at the invasive front was variable: In some invasive areas, the staining was strongly reduced, whereas in others it was heterogeneous but globally remained less intense than in the central body of the tumor (Fig. 6A, left). In the main body of HCC, E-cadherin and β-catenin localized at the plasma membrane of cancer cells. By contrast, the localization of these two epithelial markers at the plasma membrane was reduced in cancer cells of the invasive front (Fig. 6A, middle and right).

To extend the study to another type of carcinoma, we examined the expression of NM23-H1 and NM23-H2 in colorectal carcinogenesis. NM23-H1 protein was overexpressed in 8 of 10 primary colorectal carcinomas compared with adjacent control mucosa (Supplementary Fig. S11C). Overexpression appeared very early, already in tumors classified as Dukes' stages A [i.e., limited to mucosa without muscularis mucosa damage (samples 1 and 2)]. High NM23-H1 levels persisted throughout subsequent stages B2 to C2 (samples 3–10). Similar data were collected for NM23-H2. By immunohistochemical analysis, NM23-H1 protein was barely detectable in nontumoral colon epithelial cells but expressed at very high levels in colon carcinoma cells (Supplementary Fig. S11D). Remarkably, at the invasive front of colon carcinoma, NM23-H1 levels were reduced or lost (Fig. 6B, left), there was reduced E-cadherin staining at the plasma membrane, and sometimes nuclear staining of β-catenin was seen (Fig. 6B, middle and right). Interestingly, at the invasive front of this tumor, numerous single cancer cells were present with nuclear β-catenin (Fig. 6B, right, arrows). Analysis of liver and colon carcinoma samples focusing on invasive fronts deserves further investigation on a large series of tumor samples. From our silencing data and staining of NM23-H1 at the invasive front and tumors of several human liver and colon carcinoma samples, it seems that a small percentage of cancer cell populations expressing low levels of NM23-H1 protein might orchestrate the early steps of the invasive-metastatic cascade in growing primary tumors. Most importantly, the mechanisms driving the dynamic loss of NM23-H1 protein and the subsequent local tumor invasion at the early stages of carcinogenesis deserve further investigations that are currently under way in our laboratory.

Discussion

Our observations identify *NM23-H1* as the archetype of a metastasis suppressor gene acting as repressor of the early stages of the invasive program in primary tumors. We propose that NM23-H1 functions as a barrier against the conversion of *in situ* carcinoma into invasive carcinoma. Our data support the notion that *NM23-H1* silencing induces an invasive phenotype linked to partial EMT associated with the β-catenin nuclear translocation and upregulation of TCF/LEF-1–mediated transcription, a molecular signature of the Wnt pathway (32). EMT is a major switch to exacerbate the metastatic behavior by generating migratory and invasive signals, as well as anticancer drug resistance phenotypes (33). We found that NM23-H1 is reduced at the invasive front of human primary tumors concomitantly with reduced membrane-bound E-cadherin, further supporting the biological significance of our experimental data. Collectively, our data identify NM23-H1 as a critical regulator of E-cadherin–mediated intercellular adhesion in epithelial cancer cells. Consistently, NM23-H1/NM23-H2 was shown to interact and colocalize with E-cadherin, α-catenin, and γ-catenin in epithelial cancer

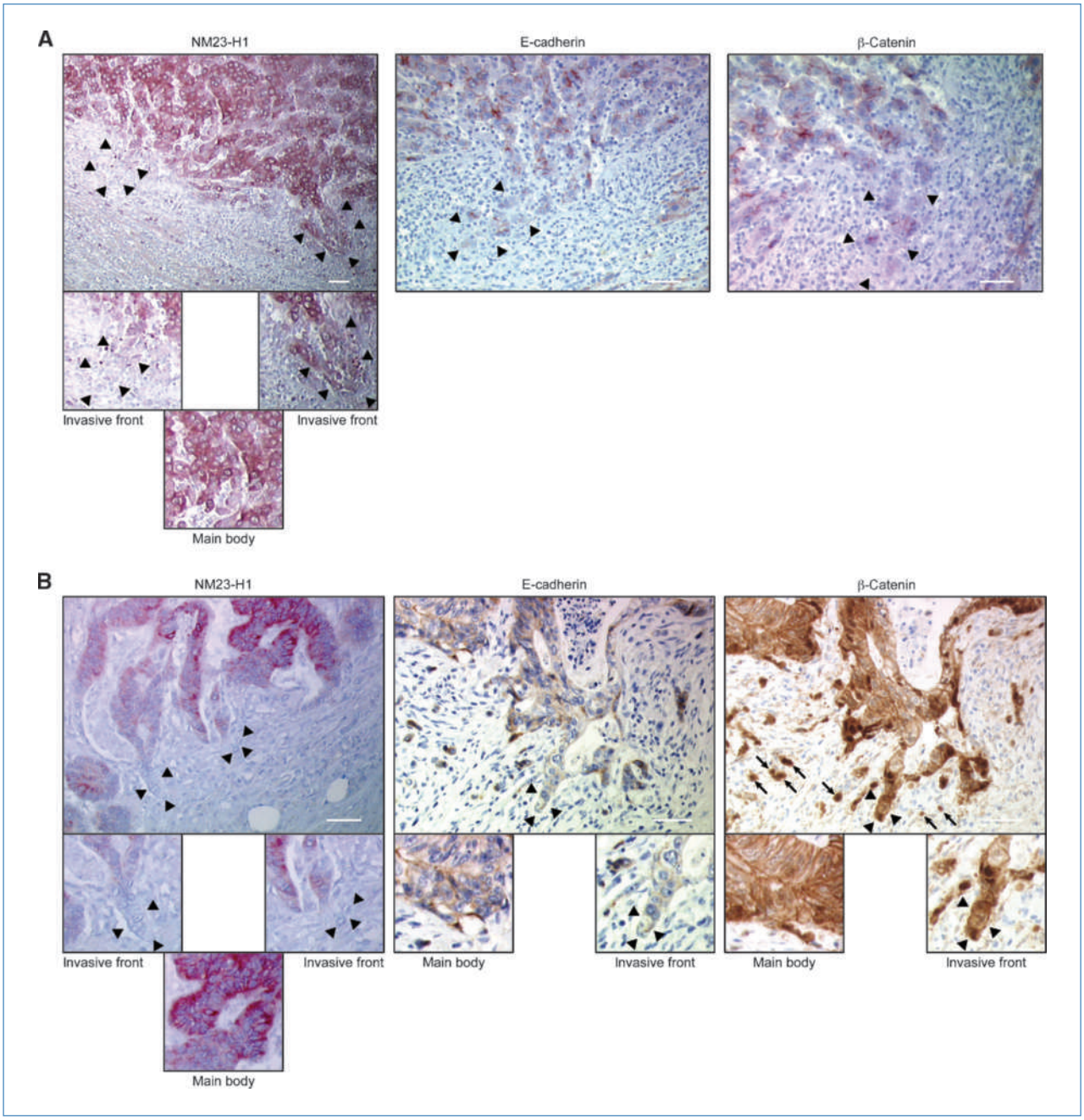

Figure 6. NM23-H1 status at the invasive front of human liver and colon tumors. Immunolabeling of NM23-H1, E-cadherin, and β-catenin in the main body and at the invasive front of human HCC (A) and colon carcinoma (B). Representative images are shown. Arrowheads show invasive fronts. In B, arrows show individual tumor cells with nuclear β-catenin. Scale bar, 50 μm.

cell lines, suggesting a role of NM23 in stabilization of junctional complexes (34).

Silenced epithelial cells display a scattered phenotype associated with increased motility and invasive activity in several matrix components (Matrigel, native type I collagen, and gelatin). Our findings suggest that NM23-H1 depletion is causally involved at early stages of the invasive program by promoting invadopodia formation and increased expression of MT1-MMP as well as MMP-1, MMP-2, MMP-3, and MMP-8 in contrast to MMP-7 and MMP-9 (data not shown), leading to matrix proteolysis. MT1-MMP degrades several ECM components, including type I, II, and III collagens, fibronectin, laminins, and fibrin, and activates pro–MMP-2, thus acting directly and indirectly as a "master regulator" of invadopodia activity and ECM remodeling (35). Also consistent with our data, one of the genes shown to be negatively

regulated by NM23-H1 is *MMP-2* (17). The unique ability of the membrane-anchored MT1-MMP rather than secreted MMPs to drive invasion is consistent with our observation that *NM23-H1* silencing is not associated with the secretion of soluble proinvasive factors (36), suggesting that the *NM23-H1* silencing–induced invasive phenotype is generated by cell-intrinsic mechanisms mediated, at least in part, by the cell surface–anchored MT1-MMP. Interestingly, invasive *NM23-H1*–silenced cells expressed high levels of TIMP-1 (data not shown). Enhanced expression of this endogenous MMP inhibitor has been linked to poor prognosis in human cancer types and was shown to promote hepatocyte growth factor/scatter factor signaling and downstream expression of MMP-2 and MMP-9 in the liver (37).

Our findings indicate a key role for NM23-H1 as a repressor of intracellular signaling pathways involved in cancer invasion. Consistently, we show that *NM23-H1* silencing induces concerted hyperactivation of MAPK modules (ERK, p38, and JNK), Rac1-GTPase, and Akt. By using selective pharmacologic inhibitors, we confirmed that these signaling elements, as well as src, PI3K, and Rho/ROCK, are required for the invasive phenotype of *NM23-H1*–silenced cells. These findings are consistent with previous studies showing that ERK signaling is repressed by NM23-H1 (38). Furthermore, considerable evidence implicates Akt hyperactivation in the EMT, cancer cell survival, invasion, and anticancer drug resistance (39). Because weak NM23-H1 expression is related to high Akt activation in ovarian carcinoma (40), our data raise the possibility that loss of NM23-H1 confers resistance to chemotherapy-induced apoptosis. We found that *NM23-H1* silencing was associated with additional activation of β-catenin–dependent TCF/LEF-1 transcription through GSK-3β–independent mechanisms. Indeed, the Wnt/TCF pathway is constitutively activated in both HepG2 and HCT8/S11 cells (30, 41). Recent studies implicate a signaling cascade using PI3K, Rac1, and JNK for β-catenin nuclear accumulation and induction of transcription (42). Taken together with our data, several lines of evidence support a model in which *NM23-H1* silencing results in activation of Tiam1, an activator of Rac1 that is repressed by NM23-H1 (12); active GTP-bound Rac1 promotes JNK activation and nuclear accumulation of β-catenin, leading to activation of Wnt target genes (43). In this connection, *NM23-H1* silencing induced MT1-MMP, a direct target of β-catenin/TCF signaling. Of note, MT1-MMP is predominantly expressed with nuclear β-catenin at the invasive front of colon carcinomas (44). Synergism between src and Wnt for transcriptional activation occurs at the AP-1 and LEF-1 response elements of the *MMP-7* promoter in HCT8/S11 cancer cells (45). In addition, src is a potent inducer of adherens junction disassembly, EMT, and cancer cell invasion. This oncogene induces MT1-MMP expression and is required for invadopodia formation to sustain efficient ECM degradation (46). Collectively, our data highlight a new signaling link between *NM23-H1* silencing and increased expression of MT1-MMP through PI3K/Akt, Rac1, JNK, and β-catenin. Therefore, it seems that *NM23-H1* silencing induces a strong invasive phenotype via multiple mechanisms, in agreement with the multifunctional properties of this metastasis suppressor protein. Moreover, we clearly established that NM23-H1 is a critical regulator of signaling networks involved in cancer cell adhesion and local invasion in primary tumors.

Adding to the complexity of the role of NM23-H1 in tumor progression, we show here a biphasic response of NM23-H1, with elevated expression in premalignant stages and primary tumors, as observed during normal liver regeneration, and subsequent reduced expression in subsets of invasive cancer cells in the stroma of primary malignant tumors. Further studies will be required to understand the mechanisms underlying this differential expression and loss of NM23-H1 during the adaptation of epithelial cancer cells within their tumor environment. This study provides a rationale for therapeutic strategies that restore or interfere with NM23-H1–regulated pathways to control the initial steps of metastatic dissemination.

Disclosure of Potential Conflicts of Interest

No potential conflicts of interest were disclosed.

Acknowledgments

We thank C. Rodrigue for assistance with the immunofluorescence analyses, S. Attoub for helpful discussion, E. Bruyneel for performing fast aggregation assays, C. Rey for technical support with partial hepatectomy, Y. Lecluse for performing flow cytometry, M. Debray for help with statistical analysis, Y. Chrétien for illustration work, and I. Yoshifumi (Imperial College London) for providing the MT1-MMP expression constructs.

Grant Support

Institut National de la Santé et de la Recherche Médicale, Université Pierre et Marie Curie, and grants (to M-L. Lacombe and C. Gespach) from the Groupement des Entreprises Françaises contre le Cancer and the Association pour la Recherche contre le Cancer (ARC-3974).

M. Boissan, C. Gespach, and M-L. Lacombe: study concept and designed research; M. Boissan, O. De Wever, F. Lizarraga, D. Wendum, R. Poincloux, and B. Nawrocki-Raby: performed research; M. Boissan, O. De Wever, F. Lizarraga, D. Wendum, R. Poincloux, S. Dufour, and B. Nawrocki-Raby: analyzed data; M. Boissan, C. Gespach, and M-L. Lacombe: wrote the paper; P. Chavrier: critical revision of the manuscript; N. Chignard, C. Desbois-Mouthon, P. Birembaut, and M. Bracke: fruitful discussion.

The costs of publication of this article were defrayed in part by the payment of page charges. This article must therefore be hereby marked *advertisement* in accordance with 18 U.S.C. Section 1734 solely to indicate this fact.

Received 05/26/2010; revised 07/27/2010; accepted 08/05/2010; published OnlineFirst 09/14/2010.

References

1. Smith SC, Theodorescu D. Learning therapeutic lessons from metastasis suppressor proteins. Nat Rev Cancer 2009;9:253–64.
2. Steeg PS, Bevilacqua G, Kopper L, et al. Evidence for a novel gene associated with low tumor metastatic potential. J Natl Cancer Inst 1988;80:200–4.
3. Boissan M, Dabernat S, Peuchant E, Schlattner U, Lascu I, Lacombe ML.

The mammalian Nm23/NDPK family: from metastasis control to cilia movement. Mol Cell Biochem 2009;329:51–62.
4. Martinez JA, Prevot S, Nordlinger B, et al. Overexpression of nm23-H1 and nm23-H2 genes in colorectal carcinomas and loss of nm23-H1 expression in advanced tumour stages. Gut 1995;37:712–20.
5. Ouatas T, Salerno M, Palmieri D, Steeg PS. Basic and translational advances in cancer metastasis: Nm23. J Bioenerg Biomembr 2003;35:73–9.
6. Lee JH, Marshall JC, Steeg PS, Horak CE. Altered gene and protein expression by Nm23-H1 in metastasis suppression. Mol Cell Biochem 2009;329:141–8.
7. Boissan M, Wendum D, Arnaud-Dabernat S, et al. Increased lung metastasis in transgenic NM23-Null/SV40 mice with hepatocellular carcinoma. J Natl Cancer Inst 2005;97:836–45.
8. MacDonald NJ, Freije JM, Stracke ML, Manrow RE, Steeg PS. Site-directed mutagenesis of nm23-H1. Mutation of proline 96 or serine 120 abrogates its motility inhibitory activity upon transfection into human breast carcinoma cells. J Biol Chem 1996;271:25107–16.
9. Leone A, Flatow U, VanHoutte K, Steeg PS. Transfection of human nm23-H1 into the human MDA-MB-435 breast carcinoma cell line: effects on tumor metastatic potential, colonization and enzymatic activity. Oncogene 1993;8:2325–33.
10. Lee HY, Lee H. Inhibitory activity of nm23-H1 on invasion and colonization of human prostate carcinoma cells is not mediated by its NDP kinase activity. Cancer Lett 1999;145:93–9.
11. Zhang Q, McCorkle J, Novak M, Yang M, Kaetzel D. Metastasis suppressor function of NM23-H1 requires its 3′;-5′ exonuclease activity. Int J Cancer, 2010 Mar 5. [Epub ahead of print].
12. Otsuki Y, Tanaka M, Yoshii S, Kawazoe N, Nakaya K, Sugimura H. Tumor metastasis suppressor nm23H1 regulates Rac1 GTPase by interaction with Tiam1. Proc Natl Acad Sci U S A 2001;98:4385–90.
13. Murakami M, Meneses PI, Knight JS, et al. Nm23-H1 modulates the activity of the guanine exchange factor Dbl-1. Int J Cancer 2008;123:500–10.
14. Horak CE, Lee JH, Elkahloun AG, et al. Nm23-H1 suppresses tumor cell motility by down-regulating the lysophosphatidic acid receptor EDG2. Cancer Res 2007;67:7238–46.
15. Hartsough MT, Morrison DK, Salerno M, et al. Nm23-H1 metastasis suppressor phosphorylation of kinase suppressor of Ras via a histidine protein kinase pathway. J Biol Chem 2002;277:32389–99.
16. Seong HA, Jung H, Ha H. NM23-H1 tumor suppressor physically interacts with serine-threonine kinase receptor-associated protein, a transforming growth factor-β (TGF-β) receptor-interacting protein, and negatively regulates TGF-β signaling. J Biol Chem 2007;282:12075–96.
17. Cheng S, Alfonso-Jaume MA, Mertens PR, Lovett DH. Tumour metastasis suppressor, nm23-β, inhibits gelatinase A transcription by interference with transactivator Y-box protein-1 (YB-1). Biochem J 2002;366:807–16.
18. Lakehal F, Dansette PM, Becquemont L, et al. Indirect cytotoxicity of flucloxacillin toward human biliary epithelium via metabolite formation in hepatocytes. Chem Res Toxicol 2001;14:694–701.
19. Vermeulen SJ, Bruyneel EA, Bracke ME, et al. Transition from the noninvasive to the invasive phenotype and loss of α-catenin in human colon cancer cells. Cancer Res 1995;55:4722–8.
20. Rivkina MB, Lunin VG, Mahov AM, Tikchonenko TI, Kukain RA. Nucleotide sequence of integrated hepatitis B virus DNA and human flanking regions in the genome of the PLC/PRF/5 cell line. Gene 1988;64:285–96.
21. Graef E, Caselmann WH, Wells J, Koshy R. Insertional activation of mevalonate kinase by hepatitis B virus DNA in a human hepatoma cell line. Oncogene 1994;9:81–7.
22. Pineau P, Marchio A, Nagamori S, Seki S, Tiollais P, Dejean A. Homozygous deletion scanning in hepatobiliary tumor cell lines reveals alternative pathways for liver carcinogenesis. Hepatology 2003;37:852–61.
23. Boterberg T, Vennekens KM, Thienpont M, Mareel MM, Bracke ME. Internalization of the E-cadherin/catenin complex and scattering of human mammary carcinoma cells MCF-7/AZ after treatment with conditioned medium from human skin squamous carcinoma cells COLO 16. Cell Adhes Commun 2000;7:299–310.
24. De Wever O, Hendrix A, De Boeck A, et al. Modeling and quantification of cancer cell invasion through collagen type I matrices. Int J Dev Biol 2010;54:887–96.
25. Fritah A, Saucier C, De Wever O, et al. Role of WISP-2/CCN5 in the maintenance of a differentiated and noninvasive phenotype in human breast cancer cells. Mol Cell Biol 2008;28:1114–23.
26. Rivat C, De Wever O, Bruyneel E, Mareel M, Gespach C, Attoub S. Disruption of STAT3 signaling leads to tumor cell invasion through alterations of homotypic cell-cell adhesion complexes. Oncogene 2004;23:3317–27.
27. Nawrocki Raby B, Polette M, Gilles C, et al. Quantitative cell dispersion analysis: new test to measure tumor cell aggressiveness. Int J Cancer 2001;93:644–52.
28. Lizarraga F, Poincloux R, Romao M, et al. Diaphanous-related formins are required for invadopodia formation and invasion of breast tumor cells. Cancer Res 2009;69:2792–800.
29. Holm S. A simple sequentially rejective multiple test procedure. Scand J Stat 1979;6:65–70.
30. de La Coste A, Romagnolo B, Billuart P, et al. Somatic mutations of the β-catenin gene are frequent in mouse and human hepatocellular carcinomas. Proc Natl Acad Sci U S A 1998;95:8847–51.
31. Radisky DC, Levy DD, Littlepage LE, et al. Rac1b and reactive oxygen species mediate MMP-3-induced EMT and genomic instability. Nature 2005;436:123–7.
32. Bienz M, Clevers H. Armadillo/β-catenin signals in the nucleus-proof beyond a reasonable doubt? Nat Cell Biol 2003;5:179–82.
33. Sabbah M, Emami S, Redeuilh G, et al. Molecular signature and therapeutic perspective of the epithelial-to-mesenchymal transitions in epithelial cancers. Drug Resist Updat 2008;11:123–51.
34. Aktary Z, Chapman K, Lam L, et al. Plakoglobin interacts with and increases the protein levels of metastasis suppressor Nm23-H2 and regulates the expression of Nm23-H1. Oncogene 2010;29:2118–29.
35. Nakahara H, Howard L, Thompson EW, et al. Transmembrane/cytoplasmic domain-mediated membrane type 1-matrix metalloprotease docking to invadopodia is required for cell invasion. Proc Natl Acad Sci U S A 1997;94:7959–64.
36. Sabeh F, Shimizu-Hirota R, Weiss SJ. Protease-dependent versus -independent cancer cell invasion programs: three-dimensional amoeboid movement revisited. J Cell Biol 2009;185:11–9.
37. Kopitz C, Gerg M, Bandapalli OR, et al. Tissue inhibitor of metalloproteinases-1 promotes liver metastasis by induction of hepatocyte growth factor signaling. Cancer Res 2007;67:8615–23.
38. Salerno M, Palmieri D, Bouadis A, Halverson D, Steeg PS. Nm23-H1 metastasis suppressor expression level influences the binding properties, stability, and function of the kinase suppressor of Ras1 (KSR1) Erk scaffold in breast carcinoma cells. Mol Cell Biol 2005;25:1379–88.
39. Grille SJ, Bellacosa A, Upson J, et al. The protein kinase Akt induces epithelial mesenchymal transition and promotes enhanced motility and invasiveness of squamous cell carcinoma lines. Cancer Res 2003;63:2172–8.
40. Hua K, Feng W, Cao Q, Zhou X, Lu X, Feng Y. Estrogen and progestin regulate metastasis through the PI3K/AKT pathway in human ovarian cancer. Int J Oncol 2008;33:959–67.
41. Le Floch N, Rivat C, De Wever O, et al. The proinvasive activity of Wnt-2 is mediated through a noncanonical Wnt pathway coupled to GSK-3β and c-Jun/AP-1 signaling. FASEB J 2005;19:144–6.
42. Wu X, Tu X, Joeng KS, Hilton MJ, Williams DA, Long F. Rac1 activation controls nuclear localization of β-catenin during canonical Wnt signaling. Cell 2008;133:340–53.
43. Esufali S, Bapat B. Cross-talk between Rac1 GTPase and dysregulated Wnt signaling pathway leads to cellular redistribution of β-catenin and TCF/LEF-mediated transcriptional activation. Oncogene 2004;23:8260–71.
44. Hlubek F, Spaderna S, Jung A, Kirchner T, Brabletz T. β-Catenin activates a coordinated expression of the proinvasive factors laminin-5 γ2 chain and MT1-MMP in colorectal carcinomas. Int J Cancer 2004;108:321–6.
45. Rivat C, Le Floch N, Sabbah M, et al. Synergistic cooperation between the AP-1 and LEF-1 transcription factors in activation of the matrilysin promoter by the src oncogene: implications in cellular invasion. FASEB J 2003;17:1721–3.
46. Bowden ET, Onikoyi E, Slack R, et al. Co-localization of cortactin and phosphotyrosine identifies active invadopodia in human breast cancer cells. Exp Cell Res 2006;312:1240–53.